Synthesis and Characterization of Functionalizable and Photopatternable Poly(ϵ-caprolactone-*co*-RS-β-malic acid)

Bin He and Mary B. Chan-Park*

The Biological and Chemical Processing Laboratory, School of Mechanical and Production Engineering, Nanyang Technological University, 50 Nanyang Avenue, 639798, Singapore

Received March 14, 2005; Revised Manuscript Received July 20, 2005

ABSTRACT: To create a functionalizable and photopatternable biodegradable polyester, 2-hydroylethyl methacrylate (HEMA) grafted poly(ϵ-caprolactone-*co*-RS-β-malic acid) (PCLMAc) was synthesized. The ring-opening random copolymerization of ϵ-caprolactone (CL) and RS-β-benzyl malolactonate (MA) using stannous octoate catalyst was systemically studied. The polymers were characterized by ^{1}H NMR, FTIR, GPC, and DSC. The optimum copolymerization temperature was found to be 130 °C. The proportion of MA in the derived copolymers was lower than that in the feeding dose, a consequence of its lower reactivity. The molecular weight of the copolymers decreased with increasing MA content. During hydrogenolysis, the protective benzyl groups were completely replaced by carboxyl groups resulting in hydrogen bonding in the deprotected copolymers, but some degradation occurred. PCL segments in the copolymers crystallized when the MA content was lower than 16.2 mol %, and the deprotected copolymer had higher crystallinity compared to that of the corresponding protected copolymer. The glass transition temperature (T_g) of the deprotected copolymer increased greatly due to the formation of hydrogen bonds. HEMA was easily grafted on the functionalized biodegradable copolymer. The liquid HEMA grafted copolymer was shown to be suitable for UV microembossing.

Introduction

Synthetic biodegradable polyesters such as poly(glycolic acid) (PGA), poly(lactic acid) (PLA), and poly(ϵ-caprolactone) (PCL) have been widely used as biomedical materials due to their excellent mechanical properties, good biocompatibility, and low toxicity.[1−4] However, these common aliphatic polyesters lack functionality necessary for some processing techniques or biomolecules immobilization, limiting their use in biomedical applications. Micropatterned tissue engineering scaffolds have been shown to be useful for the vasculature or guided nerve regeneration.[5,6] Many micropatterning techniques abound, and these include photolithography, soft lithography, and embossing. UV microembossing, a liquid micromolding technique, has been shown to be versatile and convenient.[7−9] For example, the UV microembossed films can be folded into tubular scaffolds for tissue engineering of small diameter blood vessels.[9] However, hitherto, the liquid polymers used in UV microembossing are nonbiodegradable, making the scaffolds unsuitable for tissue engineering scaffold.[7−9] Photopatternable and functionalizable biodegradable polymers are limited. To apply the UV microembossing technique to functional tissue engineering scaffold fabrication, new materials must be designed to (1) be biodegradable, (2) be a low surface tension liquid to fill and closely replicate the microcavities of the mold, and (3) have functional groups to provide cross-linking sites as well as biomolecules grafting.

Poly(β-malic acid), a synthetic biodegradable polyester with functional pendant carboxylic groups, is of great interest for biomedical applications.[10−15] The degradation product of poly(malic acid) is malic acid, which is an intermediate compound in the Krebs' cycle necessary to generate cellular energy for tissue fuel. The functionalization of biodegradable polyesters with poly(β-malic acid) has been previously reported,[27] but these are solids at room temperature. Among the synthetic biodegradable polyesters, only poly(ϵ-caprolactone) (PCL) has low T_g and T_m.[17] Since poly(malic acid) has pendant functional groups and PCL has low T_g and T_m, the random copolymer of ϵ-caprolactone and β-malic acid would combine the desired thermal properties of PCL and functional pendant groups of poly(β-malic acid) (PMAc). The random copolymer of ϵ-caprolactone and malic acid, which has not been reported thus far, could be tailored by adjusting the proportions of the two monomers in the coordination ring-opening copolymerization. The modification of functionalized biodegradable polymer would promote biospecific cell recognition and/or signaling necessary for regeneration of a multicellular organ.[18−20]

This paper reports the random copolymerization and subsequent hydrogenolysis of ϵ-caprolactone and RS-β-benzyl malolactonate to produce poly(ϵ-caprolactone-*co*-RS-β-malic acid) (PCLMAc)—a new liquid biodegradable polyester with functional pendant groups. Further, the UV microembossing of 2-hydroxyethyl methacrylate (HEMA) grafted PCLMAc is also demonstrated. In the copolymerization, the relationship between the reaction parameters (catalyst concentration, monomer ratio, and copolymerization temperature) and the copolymer properties (yield, molecular weight, polydispersity, and composition) was studied. The copolymers are characterized with nuclear magnetic resonance (NMR), Fourier transform infrared spectroscopy (FTIR), gel permeation chromatography (GPC), and differential scanning calorimetry (DSC). The UV microembossing of HEMA-*g*-PCLMAc is characterized by scanning electron microscopy (SEM).

Experimental Section

Materials. All chemicals were purchased from Aldrich. RS-bromosuccinic acid was recrystallized in acetonitrile twice;

* To whom correspondence should be addressed: e-mail mbechan@ntu.edu.sg; Tel (65) 6790 6064; Fax (65) 6792 4062.

10.1021/ma050545j CCC: $30.25
Published on Web 09/01/2005

Table 1. Copolymerization of ϵ-Caprolactone and RS-β-Benzyl Malolactonate

			MA content		mol wt of copolymer[b]			
entries	temp (°C)	$Sn(Oct)_2$	feed	polymer[a]	M_n	M_w	M_w/M_n	yield (%)
A	110	1/1000	12.2	5.9	4 700	9 700	2.06	73
B	130	1/1000	12.2	6.8	20 500	29 200	1.42	88
C	150	1/1000	12.2	7.0	13 800	21 300	1.54	85
D	170	1/1000	12.2	6.3	12 100	17 400	1.44	80
E	130	1/1000	0	0	95 700	198 000	2.07	95
F	130	1/1000	27.0	16.2	13 400	19 800	1.48	87
G	130	1/1000	45.3	35.0	10 300	14 300	1.39	82
H	130	1/1000	68.9	64.7	8 100	10 500	1.30	82
I	130	1/1000	100	100	2 900	5 700	1.97	80
J	130	1/500	12.2	6.9	19 300	28 600	1.48	87
K	130	1/2000	12.2	6.5	20 600	29 700	1.44	86

[a] Calculated from ^1H NMR measurement. [b] Determined by GPC measurement.

benzyl alcohol was used after distillation. ϵ-caprolactone (CL) was dried with sodium and distilled before use. Stannous octoate, trifluoroacetic acid anhydride (TFAA), sodium hydrogen carbonate, sodium hydroxide, magnesium sulfate, palladium on charcoal (Pd/C), and activated charcoal were used as received. *N,N′*-Dicyclohexylcarbodiimide (DCC) and 2-hydroylethyl methacrylate (HEMA) purchased were used without further purification. The photoinitiator 2,2-dimethoxy-2-phenylacetophenone was supplied as Irgacure 651 by Ciba Chemicals. Tetrahydrofuran (THF) and diethyl ether were dried with sodium and distilled. Dichloromethane, acetonitrile, chloroform, and petroleum ether were dried with calcium hydride (CaH_2) and distilled before use.

Measurement. The solvents for ^1H NMR measurement were $CDCl_3$ and acetone-d_6. The solvent contained 0.5% tetramethylsilane as the internal standard. ^1H NMR spectra were recorded on a Bruker DMX-300 spectrometer, working at 300.130 MHz. FTIR spectra were recorded on Nicolet 560 spectrometer over the wavenumber range 4000−400 cm^{-1}. Differential scanning calorimetric (DSC) measurements were made using TA DSC Q10. The procedure was as follows: first, the samples were heated to 100 °C with the heating rate of 10 °C min^{-1} (to eliminate thermal history) and then held at 100 °C for 1 min; then the samples were cooled to −80 °C with a cooling rate of 5 °C min^{-1}, held at −80 °C for 1 min, and then heated to 100 °C with a heating rate of 10 °C min^{-1}. All the scanning processes were under a nitrogen atmosphere. Molecular weight (M_n and M_w) and molecular weight distribution (M_w/M_n) were determined with respect to polystyrene standards by gel permeation chromatography (GPC), and these results were therefore used only as a qualitative tool to check the peak shape and size distribution of the different polymers. GPC was performed on an Agilent 1100 Series and analyzed with GPC−SEC data analysis software. Samples were analyzed at 25 °C with tetrahydrofuran as eluent at a flow rate of 1.0 mL min^{-1}.

Synthesis of RS-β-Benzyl Malolactonate. The synthesis of RS-β-benzyl malolactonate followed a published method.[16] 19.7 g (0.1 mol) of RS-bromosuccinic acid was dried under vacuum for 2 h, and 25 mL of THF was added under a N_2 atmosphere. The mixture was kept in an ice bath and stirred vigorously for 30 min, and 20 mL (0.14 mol) of TFAA was added slowly over 2 h. When the mixture was clear, the solvent was evaporated with a rotary evaporator, and a kind of pale yellow oil was left over. 10.8 g (0.1 mol) of distilled benzyl alcohol was added immediately, and the system was stirred vigorously at 45 °C for 12 h to give a bright yellow oil mixture. The mixture was dissolved into 100 mL of diethyl ether, washed with 100 mL of distilled water three times, and dried over $MgSO_4$/decolorizing charcoal. After filtration, the solvent in the filtrate was evaporated to yield a colorless oil product.

A solution of 2 N NaOH was added to the colorless oil slowly to adjust the pH to 7.2. The solution was heated to 45 °C, and 150 mL of benzene was added. After being stirred vigorously for 3 h, the organic phase was washed with 150 mL of 5% $NaHCO_3$ aqueous solution twice and distilled water until neutrality, and then it was dried over $MgSO_4$. After the benzene was evaporated, 5.89 g of crude RS-β-benzyl malolactonate (MA) was obtained. The crude product was purified by chromatography on silica gel twice with a solvent mixture of dichloromethane and petroleum ether (90/10).

Table 2. Variation of Compositions and Molecular Weight of Poly(ϵ-caprolactone-*co*-RS-malic acid) after Hydrogenolysis

		mol wt of copolymer[b]			
entries[c]	malic acid in PCLMAc (%)[a]	M_n	M_w	M_w/M_n	yield (%)
d-E	0	55 300	104 500	1.89	98
d-B	6.5	11 600	18 500	1.60	85
d-F	15.8	8 500	13 400	1.58	86
d-G	35.2	4 400	7 100	1.61	84
d-H	64.5	2 600	4 100	1.58	83
d-I	100	500	600	1.20	80

[a] Measured by ^1H NMR. [b] Determined by GPC measurement. [c] The corresponding entries in Table 1 were E, B, F, G, H, and I.

CL/MA Copolymerization. Prescribed amounts of CL and MA with catalyst stannous octoate were put into polymerization tubes. The tubes were degassed by several vacuum−nitrogen gas purge cycles to remove oxygen and trace water. The tubes were sealed under vacuum and placed into oil baths at different temperatures for 24 h. The polymerization tubes were broken in liquid nitrogen, and the polymers were dissolved in chloroform and then precipitated into large amounts of a mixture of diethyl ether and petroleum ether. The white protected PCLMA precipitates were dried under vacuum at room temperature for 2 days.

Hydrogenolysis. 0.2 g of Pd/C (20%) was added to a solution of 1 g of PCLMA in 100 mL of THF. The system was bubbled with H_2 and agitated continuously for 24 h. The Pd/C was filtered off and washed with THF, the merged filtrate was thickened by solvent evaporation, and the thickened solution was dropped into a large amount of diethyl ether to precipitate the deprotected copolymer. The deprotected PCLMAc precipitates were dried under vacuum at room temperature for 2 days.

HEMA Grafted PCLMAc. 11.6 g of deprotected PCLMAc (entry d-G in Table 2), 0.46 g of HEMA, and 1.33 g of DCC were added into a 100 mL bottom-rounded flask with a magnetic stirrer and 60 mL of THF. The mixture was stirred at room temperature for 24 h and filtered. The solution was condensed and precipitated in a large amount of diethyl ether. The viscous liquid was vacuum-dried at room temperature for 24 h.

UV Microembossing. 2 wt % of Irgacure 651 was added in the HEMA-*g*-PCLMAc, and the mixture was stirred at 60 °C. When Irgacure 651 was completely dissolved in the resin, the resin was dispensed onto a surface micropatterned rubber mold fabricated as previously reported.[7] The resin on the rubber mold was degassed in a vacuum at 60 °C for 30 min and then irradiated with UV for 90 s using a PK102 UV machine from I & J Fishnar Inc.; the area-averaged UV intensity at 365 nm was adjusted to be 16 mW/cm^2. The

Scheme 1. Synthetic Route of HEMA Grafted Poly(ϵ-caprolactone-*co*-RS-β-malic acid)

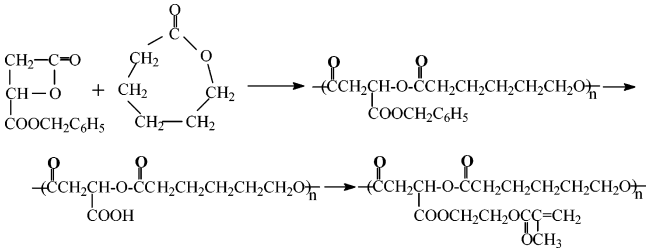

micropattern was examined using a scanning electron microscope (SEM), specifically Joel JSM-5600.

Results and Discussion

The purpose of the synthesis is to create a new functional biodegradable UV microembossing resin, which is useful in tissue engineering scaffold fabrication. The synthetic steps of HEMA grafted poly(ϵ-caprolactone-*co*-RS-β-malic acid) UV microembossing resin are shown in Scheme 1.

CL/MA Copolymerization. A catalyst is needed for the ring-opening copolymerization of ϵ-caprolactone and RS-β-benzyl malolactonate. Though the use of stannous octoate [$Sn(Oct)_2$] to catalyze the ring-opening polymerization of RS-β-benzyl malolactonate has not previously been reported, stannous octoate is an efficient and biocompatible catalyst for ring-opening polymerization of ϵ-caprolactone; therefore, we chose $Sn(Oct)_2$ to catalyze the copolymerization of ϵ-caprolactone and RS-β-benzyl malolactonate. The effects of the temperature, the monomer compositions, and the catalyst/monomer ratios were studied.

Copolymerization was attempted at a range of reaction temperatures from 90 to 170 °C with 1/1000 (molar ratio) catalyst content and 12.2% (molar ratio) MA in the feeding dose. Copolymerization failed at 90 °C but was successful at 110, 130, 150, and 170 °C, with varying copolymer properties (Table 1). The molecular weights (M_n) of the resulting copolymers were 4700, 20 500, 13 800, and 12 100 (Table 1, entries A−D). The MA proportion in the copolymers was 5.9, 6.8, 7.0, and 6.3 mol %, much lower than those in the feeding dose. Both the molecular weight and the yield were the highest at the reaction temperature of 130 °C. The polydispersity of the copolymers was 2.06, 1.42, 1.54, and 1.44, respectively. In addition to maximizing MA content, molecular weight, and yield, the 130 °C also minimized polydispersity; it was selected for further polymerization study.

With increase of the MA content in the feeding dose from 12.2 (entry B) to 27.0 (entry F), 45.3 (entry G), and 68.9 mol % (entry H), the molecular weight (M_n) of the copolymer decreased from 20 500 to 13 400, 10 300, and 8100, respectively. Variation of the MA content of the feeding dose also strongly affected the MA content of the resulting copolymers: 6.8 mol % (entry B), 16.2 mol % (entry F), 35.0 mol % (entry G), and 64.7 mol % (entry H). The MA content in the copolymer increased with the MA content in the feeding dose but at a slower rate. The variation of the molecular weight and composition demonstrates that the reactivity of ϵ-caprolactone in this copolymerization reaction is much higher than that of RS-β-benzyl malolactonate. Reaction B was repeated with varying catalyst content (entries J and K) with only modest effect on copolymer molecular weight and composition, which indicates that stannous octoate catalyzes but does not initiate the copolymerization reaction.

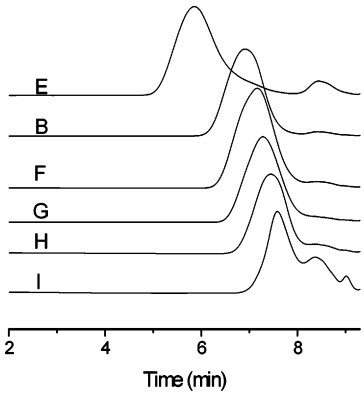

Figure 1. GPC spectra of poly(ϵ-caprolactone-*co*-RS-β-benzyl malolactonate). The polymerization conditions were 130 °C with 1/1000 catalyst concentration. The composition of MA in the copolymers was (E) 0%, (B) 6.8%, (F) 16.2%, (G) 35.0%, (H) 64.7%, and (I) 100%.

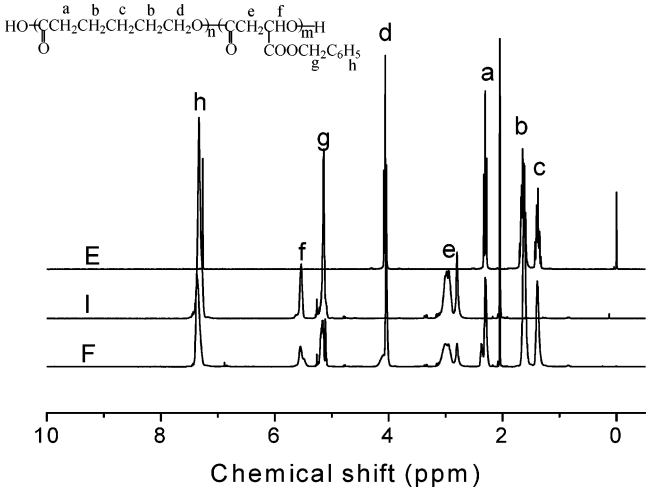

Figure 2. ^1H NMR spectra of PCL (entry E), PCLMA (entry F), and PMA (entry I). The solvent for sample E was $CDCl_3$, and the solvent for samples F and I was actone-d_6.

The GPC spectra of poly(ϵ-caprolactone-*co*-RS-β-benzyl malolactonate) are shown in Figure 1. There are residual oligomers in both the poly(ϵ-caprolactone) (entry E) and poly(RS-β-benzyl malolactonate) (entry I) homopolymers. The eluent time of the copolymer increased with increasing MA content, indicating decreased molecular weight. The calculated molecular weights using polystyrene standards are summarized in Table 1. Figure 2 shows the ^1H NMR spectra of PCL, PMA, and PCLMA. There are four different protons (h, f, g, e in Figure 2) in the MA units. They produce peaks at 7.3, 5.5, 5.2, and 2.9 ppm, respectively. The signal at 7.3 ppm (h) is due to the protons in the pendant benzene ring (C_6H_5), the signal at 5.5 ppm (f) is from the proton of C*H* in main chain, the signal of CH_2 in pendant groups appears at 5.2 ppm (g), and the signal at 2.9 ppm (e) is due to the protons of CH_2 in the main chains. The CL segment contains five proton sites. Two of these, $COCH_2CH_2CH_2$ and $CH_2CH_2CH_2O$, are in very similar chemical environments and contribute to a common signal at 1.6 ppm (b). The other three protons of $COCH_2$-CH_2 (a), $CH_2CH_2CH_2$ (c), and CH_2CH_2O (d) produce the signals at 2.4, 1.4, and 4.0 ppm. The integrated areas of the peaks of C*H* in MA at 5.5 ppm (f) and CH_2CH_2O in CL at 4.0 ppm (d) were employed to calculate the

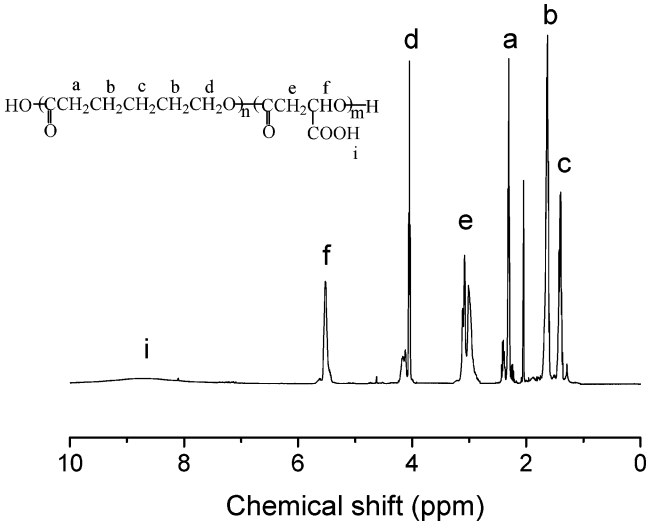

Figure 3. ^{1}H NMR spectra of poly(ϵ-caprolactone-*co*-RS-β-malic acid) (entry d-H). The solvent was actone-d_6.

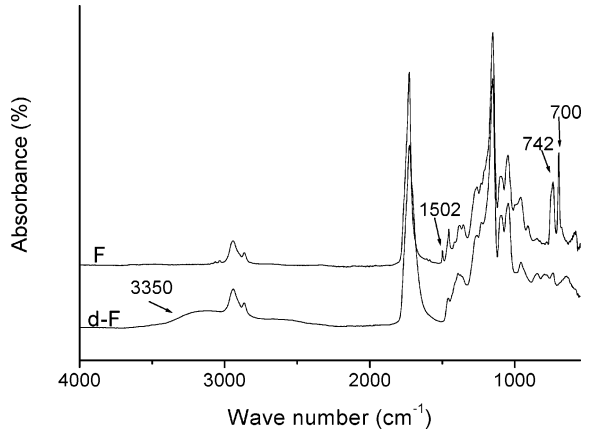

Figure 4. FTIR spectra of poly(ϵ-caprolactone-*co*-RS-β-benzyl malolactonate) (entry F) and poly(ϵ-caprolactone-*co*-RS-β-malic acid) (entry d-F). The absorbance peaks of benzene are absent, and the broad OH vibrational band of COOH is strong after hydrogenolysis.

composition of the copolymer; the derived compositions are shown in Table 1.

Hydrogenolysis. The hydrogenolysis of poly(ϵ-caprolactone-*co*-RS-β-benzyl malolactonate) was carried out in a hydrogen atmosphere with Pd/C as catalyst. The solvent was very important to the hydrogenolysis; it was needed to dissolve not only the PCLMA but also the hydrogenolysized product PCLMAc. After trials of many solvents, tetrahydrofuran was chosen as the solvent for hydrogenolysis.

The ^{1}H NMR spectrum of hydrogenolysized poly(ϵ-caprolactone-*co*-RS-β-malic acid) (entry d-H) is shown in Figure 3. It is apparent that the signals of CH_2 and C$_6H_5$ in pendant benzyl groups at 5.2 and 7.3 ppm (g and h in Figure 2) have vanished, while the other proton signals in CL and MA units are unchanged. A new wide and weak signal peak between 9.5 and 8.0 ppm (i in Figure 3) appeared and is attributed to the proton of COO*H* in pendant groups.

The FTIR spectra of PCLMA and PCLMAc are shown in Figure 4. In protected PCLMA copolymer (entry F in Table 1), the characteristic benzene ring absorbance peaks are at 700, 742, and 1502 cm^{-1} wavenumber. The deprotected PCLMAc (entry d-F of Table 2) spectrum lacks benzene ring absorbance peaks but exhibits a

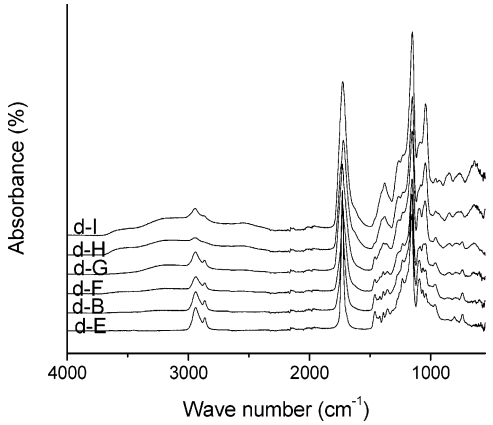

Figure 5. FTIR spectra of poly(ϵ-caprolactone-*co*-RS-β-malic acid) with malic acid content (%): (d-I) 100, (d-H) 64.5, (d-G) 35.2, (d-F) 15.8, (d-B) 6.5, and (d-E) 0.

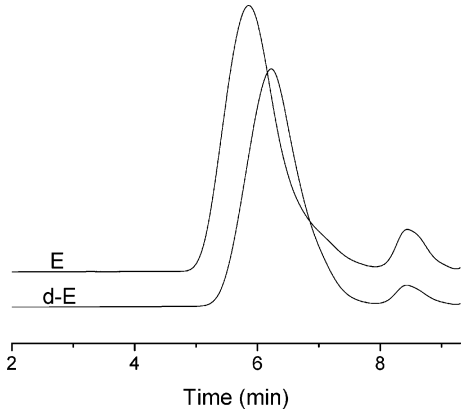

Figure 6. GPC spectra of poly(ϵ-caprolactone) before (entry E) and after (entry d-E) hydrogenolysis.

strong vibrational band, due to O−H in carboxyl groups, which extends across the wide wavenumber range 2500−3500 cm^{-1}. The changes in the spectra demonstrate that the pendant benzyl groups were changed to carboxyl groups by hydrogenolysis. Combined FTIR spectra of poly(ϵ-caprolactone-*co*-RS-β-malic acid) with β-malic acid content varying from 100, 64.5, 35.2, 15.8, 6.5 to 0 mol % are shown in Figure 5. The strong absorbance of O−H in carboxyl groups diminishes with decreasing malic acid content.

To study whether hydrogenolysis may entail degradation of the polymer chains, PCL homopolymer was hydrogenolysized at the same conditions. The molecular weight of PCL after hydrogenolysis was measured by GPC (Figure 6). The GPC spectrum shows that the molecular weight of PCL decreases after hydrogenolysis, indicating degradation in the PCL main chain.

The composition and molecular weight of PCLMAc, which was hydrogenolysized from PCLMA, are shown in Table 2. The content of malic acid in PCLMAc was nearly the same as the content of β-benzyl malolactonate in the corresponding PCLMA. The molecular weight of PCLMAc was 55 300, 11 600, 8500, 4400, 2600, and 500 for the malic acid content of 0, 6.5, 15.8, 35.2, 64.5, and 100 mol %, respectively. Each PCLMAc had a lower molecular weight than the corresponding PCLMA due to the removal of benzyl groups and the degradation of the main chain.

Thermal Properties of PCLMA and PCLMAc. Thermal properties such as T_g and T_m of the functionalized biodegradable polyesters are very important for

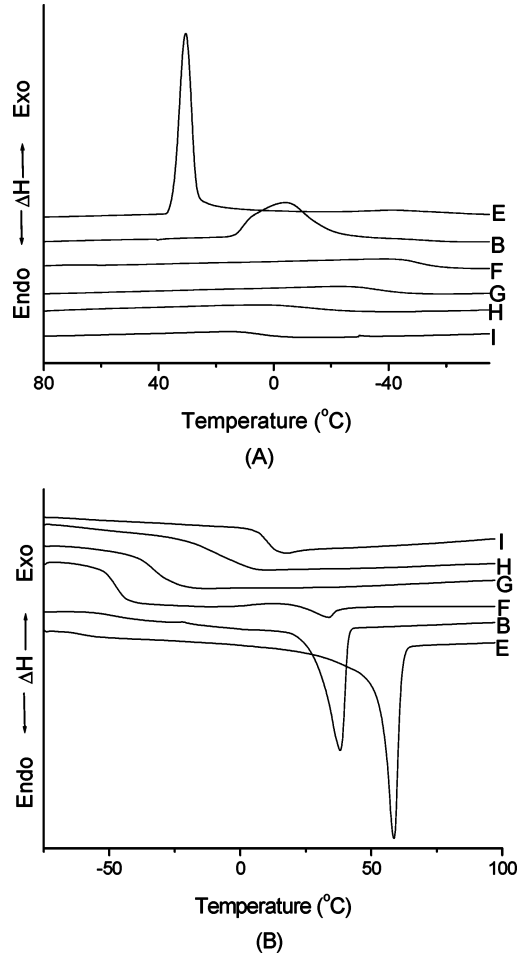

Figure 7. DSC spectra of poly(ϵ-caprolactone-*co*-RS-β-benzyl malolactonate): (A) with cooling temperature rate 5 °C/min; (B) with heating temperature rate 10 °C/min. The MA content (%) was (E) 0, (B) 6.8, (F) 16.2, (G) 35.0, (H) 64.7, and (I) 100.

Table 3. Thermal Properties of Poly(ϵ-caprolactone-*co*-RS-β-benzyl malolactonate) and Poly((ϵ-caprolactone-*co*-RS-β-malic acid)[a]

	T_g (°C)		T_c (°C)		T_m (°C)		ΔH (J/g)	
entries	P1[b]	P2[c]	P1[b]	P2[c]	P1[b]	P2[c]	P1[b]	P2[c]
E/d-E	−56	−57	31	31	59	58	54.06	61.24
B/d-B	−49	−38	−4	7	38	43 (38)	37.15	40.31
F/d-F	−43	−33			23		1.69	
G/d-G	−25	−5						
H/d-H	5	26						
I/d-I	14	33						

[a] Determined by GPC measurement. [b] PCLMA. [c] PCLMAc.

processability. Figure 7 shows the DSC spectra of PCLMA with different MA content. Figure 7A shows the spectra of the cooling process from 100 to −80 °C. The copolymer (entry B) with 6.8 mol % MA content crystallized, but the crystallization peak is much wider and weaker than that of PCL homopolymer (entry E). No crystallization peaks appeared when the MA content was increased from 16.2 (entry F) to 100% (entry I). The absence of crystallinity in the higher MA content copolymers (Table 3) is attributed to the disruption of the regularity of PCL and its large sterically hindrant benzyl pendant groups. Figure 7B shows the thermal behavior of PCLMA in the heating process as the temperature increases from −80 to 100 °C. Three copolymers, entries E, B, and F, have endothermal melting peaks; the peak in entry F is very weak. The

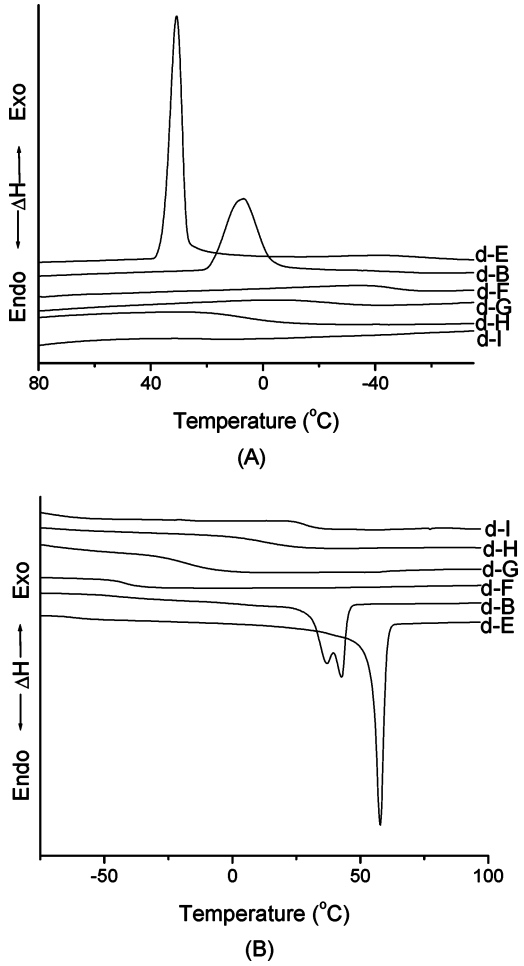

Figure 8. DSC spectra of poly(ϵ-caprolactone-*co*-RS-β-malic acid): (A) with cooling temperature rate 5 °C/min; (B) with heating temperature rate 10 °C/min. The malic acid content (%) was (E) 0, (B) 6.5, (F) 15.8, (G) 35.2, (H) 64.5, and (I) 100.

DSC spectra of PCLMAc during the cooling and heating processes are shown in Figure 8. Like the spectra in Figure 7A, crystallization peaks appear in the entries d-E and d-B, which are the corresponding copolymers to entries E and B. There are some differences between the deprotected and protected copolymer scans. The exothermal crystallization peak of entry d-B in Figure 8A is much sharper than that of entry B in Figure 7A. The weak endothermal melting peak of the entry F heating scan (Figure 7B) is absent in d-F (Figure 8B), and the endothermal melting peak in entry d-B is split into two peaks, a weaker peak at 38 °C and a stronger peak at 43 °C.

The thermal properties of PCLMA and PCLMAc are summarized in Table 3. The glass transition temperature (T_g) of both PCLMA and PCLMAc increases when MA content increases from 0 to 100 mol % (Table 3). The T_g of PCLMA is −56 °C (entry E), −49 °C (entry B), −43 °C (entry F), −25 °C (entry G), 5 °C (entry H), and 14 °C (entry I) with the corresponding MA content of 0, 6.5, 15.8, 35.2, 64.5, and 100 mol %, respectively. The T_g of corresponding PCLMAc is −57 °C (entry d-E), −38 °C (entry d-B), −33 °C (entry d-F), −5 °C (entry d-G), 26 °C (entry d-H), and 33 °C (entry d-I). PCL homopolymer is a semicrystalline polymer with T_g of −56 °C (entry E, Table 3). Poly(RS-β-benzyl malolactonate) (PMA) homopolymer is an amorphous polymer with T_g of 14 °C (entry I, Table 3). The T_g of PMA is higher than that of PCL, so the increase of PCLMA T_g

with MA content is expected. Similarly, the T_g of PMAc homopolymer is 33 °C, higher than PCL homopolymer, leading to the higher T_g of PCLMAc copolymer with increased MAc content. Both the protected and deprotected copolymers exhibit a single glass transition temperature, demonstrating that these polymers are indeed copolymers of ϵ-caprolactone and RS-β-benzyl malolactonate or RS-β-benzyl malic acid rather than mixtures of the homopolymers of poly(ϵ-caprolactone) and poly(RS-β-benzyl malolactonate) or poly(RS-β-benzyl malic acid). DSC results show that all the functionalized copolymers are liquid at 50 °C. These materials are potentially suitable for tissue engineering scaffold fabrication by UV microembossing.

The inter- and intramolecular interactions of PCLMAc and PCLMA are different. The pendant carboxyl groups of PCLMAc have small steric hindrance compared to benzyl groups of PCLMA. In PCLMAc, inter- and intramolecular hydrogen bonds exist between pendant carboxyl groups. These hydrogen bonds strengthen the interaction between polymeric chains. This accounts for the higher T_g, T_m, and ΔH of PCLMAc compared to those of the corresponding PCLMA (Table 3) and the sharper exothermal peak of PCLMAc (entry d-B) than that of PCLMA (entry B). The appearance of two endothermal peaks in entry d-B is also attributed to the formation of hydrogen bonds.[16] The hydrogen bonds hamper the movement of the main chains and limit them in certain domains; thus, PCL segments in copolymer crystallize imperfectly in these domains. The imperfect PCL crystals lead to two endothermic peaks.

The degradation in hydrogenolysis also affects the crystallization of PCLMAc. The molecular weight (M_n) of PCL homopolymer decreases from 95 700 (entry E, Table 1) to 55 300 (entry d-E, Table 2) with hydrogenolysis. The ΔH of PCL increases from 54.06 J/g (entry E) to 61.24 J/g (entry d-E) due to the increased mobility of PCL chains of lower molecular weight (Table 3). Similarly, the ΔH of PCLMA (entry B) increases from 37.15 to 40.31 J/g after removal of the benzyl groups. The disappearance of an endothermal melting peak in entry d-F is also attributed to the degradation that occurs in hydrogenolysis; the degradation lowers the molecular weight of copolymer so much that it can no longer crystallize (Figure 8B).

FTIR is an effective method for the study of polymer interactions, especially hydrogen bonding.[21−24] This technique was applied to our new copolymers to better characterize their structure. FTIR spectra were obtained at a range of temperatures from room temperature (about 22 °C) to 100 °C. The FTIR spectra of the O−H stretching band of PCLMAc are shown in Figure 9. The free vibrations of O−H around 3500 cm^{-1} weaken and the H-bonded O−H vibrations strengthen around 3200 cm^{-1} as the temperature increases from 22 to 100 °C in PCLMAc d-I. There is no change with temperature in PCLMAc d-G. The observed behaviors of the spectra are attributed to the glass transition. Below the glass transition temperature, the polymeric chains are frozen, the pendant functional groups cannot move freely, and it is more difficult for O−H groups to form hydrogen bonds, so that their IR absorbance peaks appear around 3500 cm^{-1}. At temperatures above T_g, the copolymer is in an elastic state, the mobility of polymeric chains is enhanced, and more hydrogen bonds are formed, so that the IR absorbance in the H-bonded O−H stretching band around 3200 cm^{-1} is strengthened. The glass

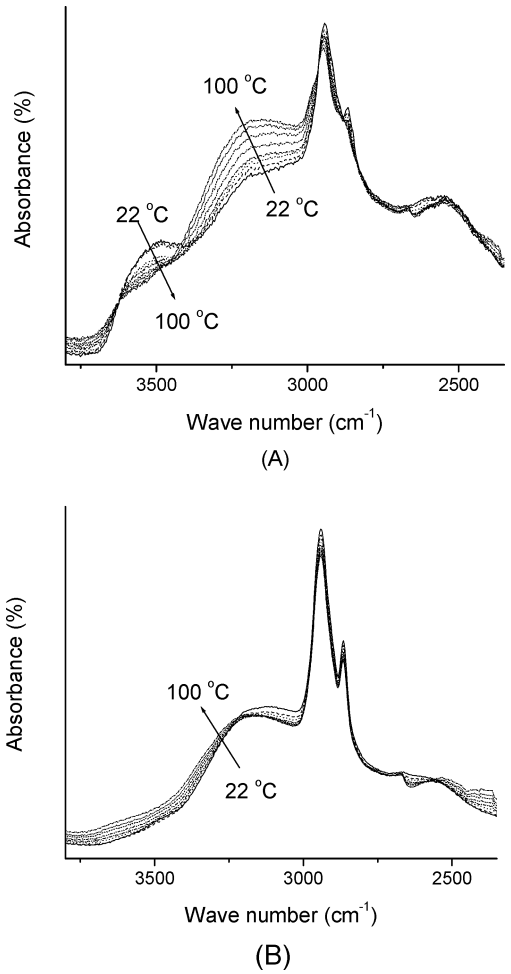

Figure 9. Temperature-dependent FTIR spectra of O−H stretching region in poly(ϵ-caprolactone-*co*-RS-β-malic acid): (A) entry d-I; (B) entry d-G.

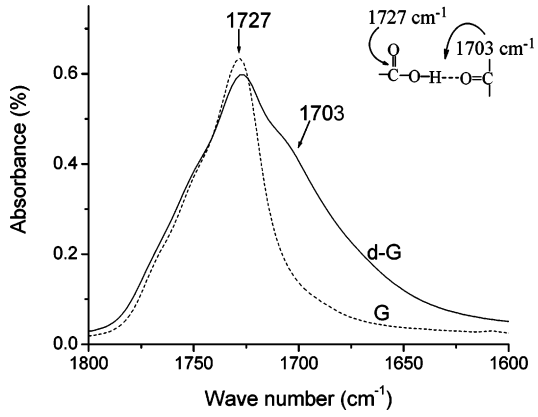

Figure 10. FTIR spectra of the carbonyl region in poly(ϵ-caprolactone-*co*-RS-β-benzyl malolactonate) (G) and poly(ϵ-caprolactone-*co*-RS-β-malic acid) (d-G).

transition temperature of PCLMAc d-I is 33 °C, and its IR absorbance spectra in the O−H band exhibit changes in keeping with the above interpretation. The glass transition temperature of PCLMAc d-G is −5 °C, below the lowest temperature at which spectra were obtained, and the O−H band spectra exhibit essentially no variation with temperature.

The FTIR spectra of the carbonyl region (C=O) in PCLMA (entry G) and PCLMAc (entry d-G) are presented in Figure 10. There is one peak at 1727 cm^{-1} in protected PCLMA. A shoulder peak at 1703 cm^{-1}

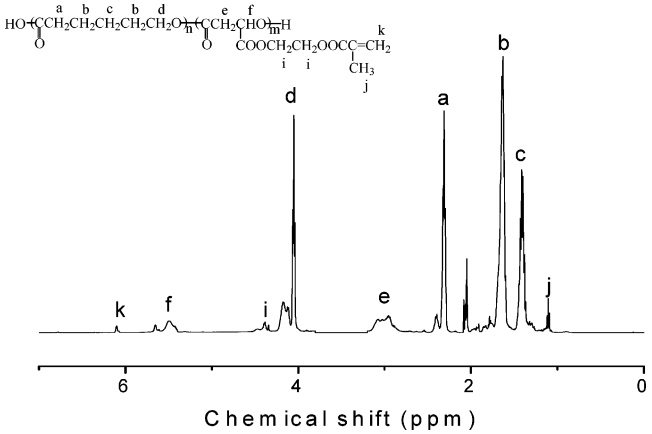

Figure 11. ^{1}H NMR spectra of HEMA grafted poly(ϵ-caprolactone-*co*-RS-β-malic acid).

appears in the deprotected PCLMAc. The two C=O vibrational peaks centered at 1727 and 1703 cm^{-1} are attributed to vibration of free and hydrogen-bonded carbonyl groups, respectively. Since malic acid with carboxylic acid group is the minor constituent, there are not enough OH groups to form hydrogen bonds with all carbonyl groups. Therefore, both free and hydrogen-bonded carbonyl groups exist in deprotected PCLMAc.

UV Microembossing of HEMA-*g*-PCLMAc. The ^{1}H NMR of HEMA grafted PCLMAc is shown in Figure 11. Comparing with the ^{1}H NMR of PLMAc, it is obvious that three new peaks appeared at 6.10 (k), 4.38 (i), and 1.10 ppm (j). They are attributed to the protons of C=CH_2, CH_2CH_2, and −CH_3 in HEMA. Because of the effect of unsaturated carbon double bond, the protons in C=CH_2 split into several peaks, which were located at 6.10 and 5.65 ppm (at the left of peak f). The protons in CH_2CH_2 also split into multipeaks located from 4.30 to 4.55 ppm. The intensity of peak j was chosen to calculate the content of HEMA grafting, and 10% of β-malic acid was grafted HEMA, which coincided with the feeding dose. It means that the efficiency of HEMA grafting was very high with DCC as catalyst. The malic acid content in d-G is 35.2% (Table 2), making the content of HEMA in the total polymer to be 3.5%.

The UV microembossing of HEMA-*g*-PCLMAc was carried out under UV irradiation with 2% Irgacure 651 as photoinitiator. Two molds PDMS rubbers were used as molds for UV embossing. The micropatterns fabricated were 120 × 60 × 25 and 80 × 60 × 25 μm (channel width by channel depth by wall width). The SEMs of UV microembossed HEMA-*g*-PCLMAc are shown in Figure 12. The resin filled the microcavities, replicated the mold, and cured well and has sufficient mechanical strength to enable demolding without distortion.

Conclusion

We synthesized a functionalizable and photopatternable HEMA grafted poly(ϵ-caprolactone-*co*-RS-β-malic acid) resin. The random ring-opening copolymerization of ϵ-caprolactone and RS-β-benzyl malolactonate using stannous octoate catalyst to produce liquid polymers

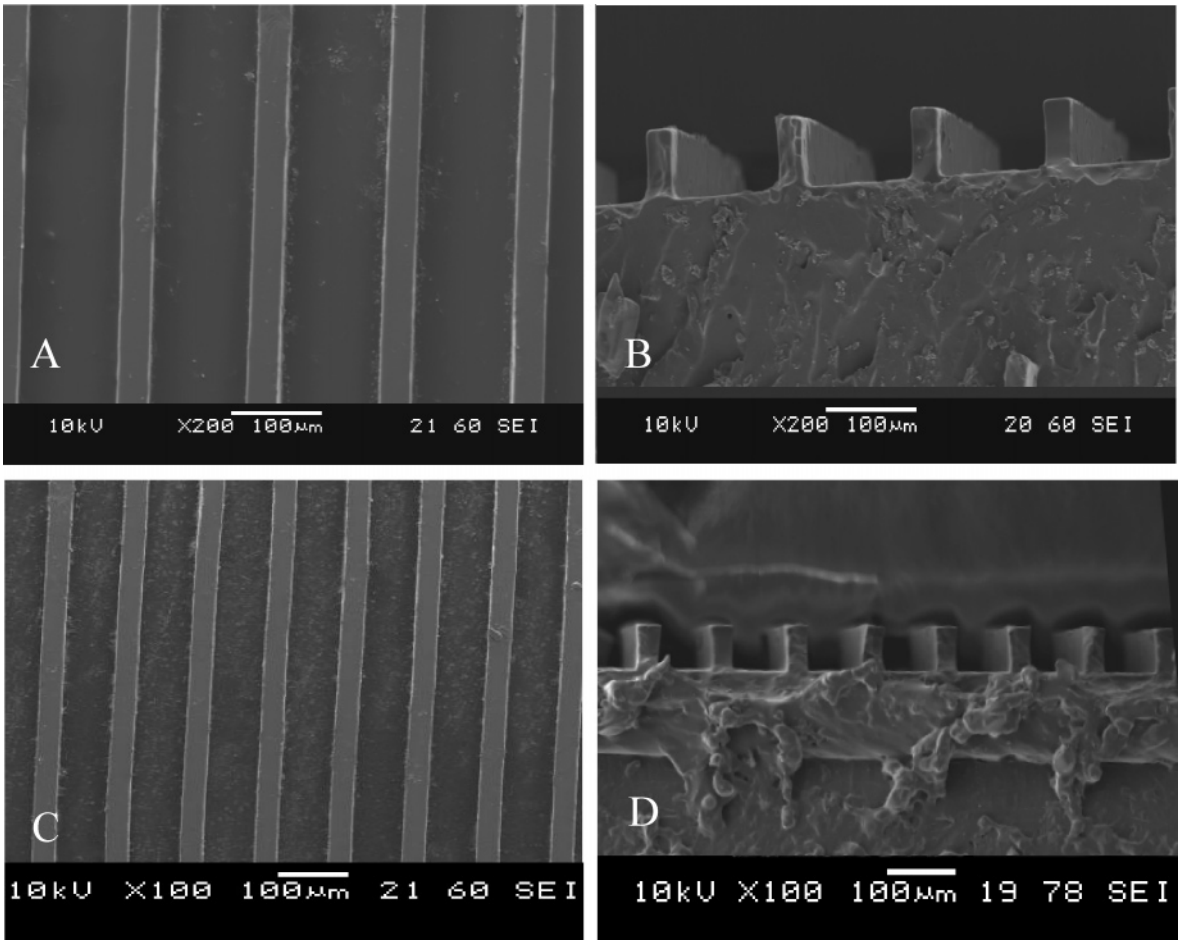

Figure 12. UV-microembossing SEM of HEMA grafted poly(ϵ-caprolactone-*co*-RS-β-malic acid). (A) and (B) are surface and cross section of UV microembossing with 120 μm channel width, 60 μm depth, and 25 μm wall width. (C) and (D) are surface and cross section of UV microembossing with 80 μm channel width, 60 μm depth, and 25 μm wall width.

was systemically studied. The reactivity of ϵ-caprolactone in copolymerization was higher than that of RS-β-benzyl malolactonate. The molecular weight and glass transition temperature (T_g) of the copolymers decreased with increasing ϵ-caprolactone content. The protective benzyl groups were removed completely in hydrogenolysis, but some main chain degradation occurred. FTIR spectra showed that hydrogen bonds formed in the functionalized copolymers. The T_g, T_c, and T_m of PCLMAc were higher than those of corresponding PCLMA due to the hydrogen bonds in PCLMAc. The liquid HEMA grafted poly(ϵ-caprolactone-*co*-RS-β-malic acid) was shown to be a suitable liquid resin for UV microembossing. It has potential applications in tissue engineering scaffold fabrication.

Acknowledgment. This research was supported by an A-STAR (Singapore) grant (Project No. 022 107 0004).

References and Notes

(1) Kulkarni, R. K.; Pani, K. C.; Neuman, C.; Leonard, F. *Arch. Surg.* **1966**, *93*, 839.
(2) Gilding, D. K.; Reed, A. M. *Polymer* **1979**, *20*, 1459.
(3) Gilding, D. K.; Reed, A. M. *J. Biomed. Mater. Res.* **1971**, *5*, 169.
(4) Pulapura, S.; Kohn, J. *J. Biomater. Appl.* **1992**, *6*, 216.
(5) Shin, M.; Matsuda, K.; Ishii, O.; Terai, H.; Kaazempur-Mofrad, M.; Borenstein, J.; Detmar, M.; Vacanti, J. P. *Biomed. Microdevices* **2004**, *6*, 269.
(6) Thompson, D. M.; Buettner, H. M. *Tissue Eng.* **2001**, *7*, 247.
(7) Yan, Y. H.; Chan-Park, M. B.; Gao, J. X.; Yue, C. Y. *Langmuir* **2004**, *20*, 1031.
(8) Chan-Park, M. B.; Yan, Y. H.; Neo, W. K.; Zhou, W. X.; Zhang, J.; Yue, C. Y. *Langmuir* **2003**, *19*, 4371.
(9) Jin, Y.; Shen, M. B.; Chan-Park, Z. Q.; Feng, V. C.; Zhi W. F. *J. Biomed. Mater. Res. B*, in press.
(10) Bear, M. M.; Lozac'h, K.; Randriamahefa, S.; Langlois, V.; Bourbouze, R.; Guerin, P. *Polymer* **1999**, *40*, 6521.
(11) Osanai, S.; Nakamura, K. *Biomaterials* **2000**, *21*, 867.
(12) Vert, M. *Polym. Degrad. Stab.* **1998**, *59*, 169.
(13) Bizzarri, R.; Chiellini, F.; Solaro, R.; Chiellini, E.; Camass, S.; Guerin, P. *Macromolecules* **2002**, *35*, 1215.
(14) Coulembier, O.; Degee, P.; Cammas, S.; Guerin, P.; Dubois, P. *Macromolecules* **2002**, *35*, 9896.
(15) He, B.; Wan, Y.; Bei, J. Z.; Wang, S. G. *Biomaterials* **2004**, *25*, 5239.
(16) He, B.; Bei, J. Z.; Wang, S. G. *Polymer* **2003**, 44, 989.
(17) Kuo, S. W.; Lin, C. L.; Chang, F. C. *Macromolecules* **2002**, *35*, 278.
(18) Hubbell, J. A. *Curr. Opin. Biotech.* **1999**, *10*, 123.
(19) Langer, R. *J. Controlled Release* **1999**, *62*, 7.
(20) Yamaoka, T.; Hotta, Y.; Kobayashi, K.; Kimura, Y. *Int. J. Biol. Macromol.* **1992**, *25*, 265.
(21) Sato, H.; Murakami, R.; Padermshoke, A.; Hirose, F.; Senda, K.; Noda, I.; Ozaki, Y. *Macromolecules* **2004**, *37*, 7203.
(22) Iriondo, P.; Iruin, J. J.; Fernandez-Berridi, M. J. *Macromolecules* **1996**, *29*, 5605.
(23) Dong, J.; Ozaki, Y. *Macromolecules* **1997**, *30*, 286.
(24) Li, D.; Brisson, J. *Macromolecules* **1996**, *29*, 868.

MA050545J